J. metamorphic Geol. 1988, **6**, 721–724

Author Index

Audren, Cl., *see* Triboulet, Cl.
Ballèvre, M., *see* Reynard, B.
Barbey, P., *see* Boullier, A.-M.
Barnes, S.-J., *see* Sawyer, E.W.
Barnicoat, A.C. The mechanism of veining and retrograde alteration of Alpine eclogites, 545.
Bell, T.H., *see* Rubenach, M.J.
Bevins, R.E. & Merriman, R.J. Compositional controls on coexisting prehnite–actinolite and prehnite–pumpellyite facies assemblages in the Tal y Fan metabasite intrusion, North Wales: implications for Caledonian metamorphic field gradients, 17.
Blenkinsop, T.G. Definition of low-grade metamorphic zones using illite crystallinity, 613.
van Bosse, J.Y. & Williams-Jones, A.E. Chemographic relationships of biotite and cordierite in the McGerrigle thermal aureole, Gaspé, Quebec, 65.
Boullier, A.-M. & Barbey, P. A polycyclic two-stage corona growth in the Iforas Granulitic Unit (Mali), 235.
Bucher-Nurminen, K. Compositional variation of phlogopite in a marble sample: iimplications for geological thermobarometry, 667.
Cartwright, I. Crystallization of melts, pegmatite intrusion and the Inverian retrogression of the Scourian complex, north-west Scotland, 77.
Craw, D. Shallow-level metamorphic fluids in a high uplift rate metamorphic belt; Alpine Schist, New Zealand, 1.
Currie, K.L. & Gittins, J. Contrasting sapphirine parageneses from Wilson Lake, Labrador and their tectonic implications, 593.
Day, H.W., *see* Tracy, R.J.
Dell'Angelo, L.N. & Tullis, J. Experimental deformation of partially melted granitic aggregates, 495.
Dickenson, M.P. Local and regional differences in the chemical potential of water in amphibolite facies pelitic schists, 365.
Duebendorfer, E.M. Evidence for an inverted metamorphic gradient associated with a Precambrian suture, southern Wyoming, 41.
Forest, R.C., *see* Hynes, A.
Gittins, J., *see* Currie, K.L.
Godard, G., *see* Thieblemont, D.
Harte, B., *see* Pattison, D.R.M.
Holland, T.J.B., *see* Powell, R.
Hollister, L.S. On the origin of CO_2-rich fluid inclusions in migmatites, 467.
Hynes, A. & Forest, R.C. Empirical garnet–muscovite geothermometry in low-grade metapelites, Selwyn Range (Canadian Rockies), 297.
Johannes, W. What controls partial melting in migmatites? 451.
Karabinos, P. & Ketcham, R. Thermal structure of active thrust belts, 559.
Ketcham, R., *see* Karabinos, P.
Kwak, T.A.P., *see* Wright, J.H.
McDougall, I, *see* Wijbrans, J.R.
McLellan, E.L. Migmatite structures in the Central Gneiss Comples, Boca de Quadra, Alaska, 517.
Martin, S.F., *see* Sandiford, M.
Martingnole, J., *see* Perreault, S.
Merriman, R.J., *see* Bevins, R.E.
de Nooy, D., *see* Phillips, G.N.
Pattison, D.R.M. & Harte, B. Evolution of structurally contrasting anatectic migmatites in the 3-kbar Ballachulish aureole, Scotland, 475.
Perera, L.R.K., *see* Sandiford, M.
Perreault, S. & Martingnole, J. High-temperature cordierite migmatites in the north-eastern Grenville province, 673.
Phillips, G.N. Widespread fluid infiltration during metamorphism of the Witwatersrand goldfields: generation of chloritoid and pyrophyllite, 311.
Phillips, G.N. & de Nooy, D. High-grade metamorphic processes which influence Archaean gold deposits, with particular reference to Big Bell, Australia, 95.
Powell, R. & Holland, T.J.B. An internally consistent dataset with uncertainties and correlations: 3. Applications to geobarometry, worked examples and a computer program, 173.
Powell, R., *see* Sandiford, M.
Reynard, B. & Ballèvre, M. Coexisting amphiboles in an eclogite from the western Alps: new constraints on the miscibility gap between sodic and calcic amphiboles, 333.
Rice, A.H.N. & Roberts, D. Multi-textured garnets from a single growth event: an example from northern Norway, 159.
Roberts, D., *see* Rice, A.H.N.
Rubenach, M.J. & Bell, T.H. Micro-structural controls and the role of graphite in matrix/porphyroblast exchange during synkinematic andalusite growth in a granitoid aureole, 651.
Sandiford, M., Powell, R., Martin, S.F. & Perera, L.R.K. Thermal and baric evolution of garnet granulites from Sri Lanka, 351.
Sawyer, E.W. & Barnes, S.-J. Temporal and compositional differences between subsolidus and anatectic migmatite leucosomes from the Quetico metasedimentary belt, Canada, 437.
Sedlock, R.L. Metamorphic petrology of a high-pressure, low-temperature subduction complex in west-central Baja California, Mexico, 205.
Shiba, M. Metamorphic evolution of the southern part of the Hidaka belt, Hokkaido, Japan, 273.
Sorensen, S.S. Petrology of amphibolite-facies mafic and ultramafic rocks from the Catalina Schist, southern California: metasomatism and migmatization in a subduction zone metamorphic setting, 405.
Thieblemont, D., Triboulet, C. & Godard, G. Mineralogy, petrology and *P–T–t* path of Ca–Na amphibole assemblages, Saint-Martin des Noyers formation, Vendée, France, 697.
Tracy, R.J. & Day, H.W. Studies in the genesis and deformation of migmatites: introduction, 385.
Triboulet, Cl. & Audren, Cl. Controls on *P–T–t* deformation path from amphibole zonation during

progressive metamorphism of basic rocks (estuary of the River Vilaine, South Brittany, France), 117.
Triboulet, C., *see* Thieblemont, D.
Tullis, J., *see* Dell'Angelo, L.N.
Vernon, R.H. Microstructural evidence of rotation and non-rotation of mica porphyroblasts, 585.
Vernon, R.H. Sequential growth of cordierite and andalusite porphyroblasts, Cooma Complex, Australia: microstructural evidence of a prograde reaction, 255.
Vuichard, J.P. & Ballèvre, M. Garnet–chloritoid equilibria in eclogitic pelitic rocks from the Sesia zone (Western Alps): their bearing on phase relations in high pressure metapelites, 135.
Waters, D.J. Partial melting and the formation of granulite facies assemblages in Namaqualand, South Africa, 387.
Wijbrans, J.R. & McDougall, I. Metamorphic evolution of the Attic Cycladic Metamorphic Belt on Naxos (Cyclades, Greece) utilizing $^{40}Ar/^{39}Ar$ age spectrum measurements, 571.
Williams-Jones, A.E., *see* van Bosse, J.Y.
Wright, J.H. & Kwak, T.A.P. Endogreisen, brecciation and fluid activity at the Mount Bischoff Sn-deposit, north-west Tasmania, Australia, 629.

Subject Index

Alpine Fault, 1
alteration, 95, 311, 545
amphiboles, 333, 697
amphibole solvus, 697
amphibolite, 95, 405, 697
anatectic leucosome, 437
anatexis, 475
anchizone, 623
andalusite, 255
andalusite–sillimanite type metamorphism, 273
Archaean, 437
$^{40}Ar/^{39}Ar$ geochronology, 571
Attic Cycladic Metamorphic Belt, 571

Baja California, 205
Ballachulish aureole, Scotland, 475
barroisite, 697
Big Bell, 95
biotite, 159, 595
biotite–cordierite equilibria, 65
blueschists, 205
brines, 1
buffering of water activity, 387
bulk geochemical changes, 629

Caledonian metamorphism, 17
Caledonides, 159
Canada, 297
chemical potential, 365
chemistry, 451
chloritoid, 311
compositional controls, 17
computer program, 173
contact metamorphism, 65, 475
Cooma Complex, south-east Australia, 255
cordierite, 255, 673
cordierite-bearing pegmatites, 673
critical melt fraction, 475
crystallization of melts, 77

deformation, 495
deformation mechanisms, 495
diagenetic, 623

Eburnean orogeny, 235
eclogite, 333
endogreisens, 629
epizone, 623
exogreisens, 629

fluid absent, 545
fluid inclusions, 1, 467, 629

garnet, 159, 297, 697
garnet–chloritoid, 135
geobarometry, 173, 697
geothermobarometry, 235, 673
geothermometry, 173, 297, 697
gold, 95, 311
Gondwana, 351
granite, 495
granulite facies, 77, 387
granulites, 351, 603

Hercynian orogeny, 117
heterogeneous strain, 595
Hidaka metamorphic belt, 273
high-pressure metamorphism, 135
hydraulic fracture, 545

illite crystallinity, 623
infiltration, 311, 365
Inverian retrogression, 77
inverted metamorphic gradient, 41
island arc-system, 697
isothermal decompression, 603

jadeitic clinopyroxene, 205

leucosomes, 673

mafic migmatite, 405
marbles, 667
McGerrigle aureole, Quebec, Canada, 65
melting, 95
melt segregation, 517
mesosomes, 673
metamorphic fluids, 1
metamorphic terrane, 405
metapelites, 41, 135, 297
metasomatism, 405
mica, 595
microstructures, 117, 495
migmatite geochemistry, 437
migmatites, 474, 475
migmatite structures, 517
miscibility gaps, 333
Moosilauke area NH, USA, 365
muscovite, 297, 595

Namaqualand Metamorphic Complex, 387
New Zealand, 1
non-equilibrium phlogopite compositions, 667
non-rotation, 595
north-west Scotland, 77
Norway, 159

orogenic belt, 273

Pan-African orogeny, 235
partial melt, 495
partial melting, 387, 451
pegmatite intrusion, 77
pelite, 311
phengite, 297
polymetamorphism, 235
porphyroblast-matrix exchange, 651
porphyroblasts, 255, 595
Precambrian suture, 41
prehnite–actinolite facies, 17
prehnite–pumpellyite facies, 17
Proterozoic, 603
P–T–t–d paths, 117
P–T–t path, 235, 273
pyrophyllite, 311

Quetico Metasedimentary Belt, 437

reaction veins, 667
replacement, 159
role of graphite, 651
rotation, 595

Saint-Augustin, Grenville province, 673
sapphirine, 603
Scourian complex, 77
Sesia zone, 135
sequential growth, 255
shale, 311
shear bands, 517
skeletal growth, 651
South Brittany, France, 117
Sri Lanka, 351
stacking effect during collision processes, 117
stromatic migmatites, 451
subduction, 205
subduction zone, 405
subsolidus leucosome, 437
Superior Province, 437
symplectite textures, 351
syndeformational growth, 255
synkinematic andalusite, 651
synmigmatization stresses, 517

Taconian orogeny, 559
textures, 159
thermal and tectonic history, 571
thermal aspects, 41
thermal modelling, 559
thermobarometry, 667
thermodynamic analysis, 365
thermodynamic calculations, 173
thermodynamic dataset, 173
thrust belts, 559
thrust systems, 41
tin deposit, 629
tremolite/ededite/magnesio-hornblende equilibria, 117

uplift, 205

vein networks, 517
Vendée, France, 697
volume change, 517

Wales, UK, 17
water, 365
Western Alps, 135, 333
Wilson Lake, Labrador, 603
Witwatersrand, 311
wollastonite, 351
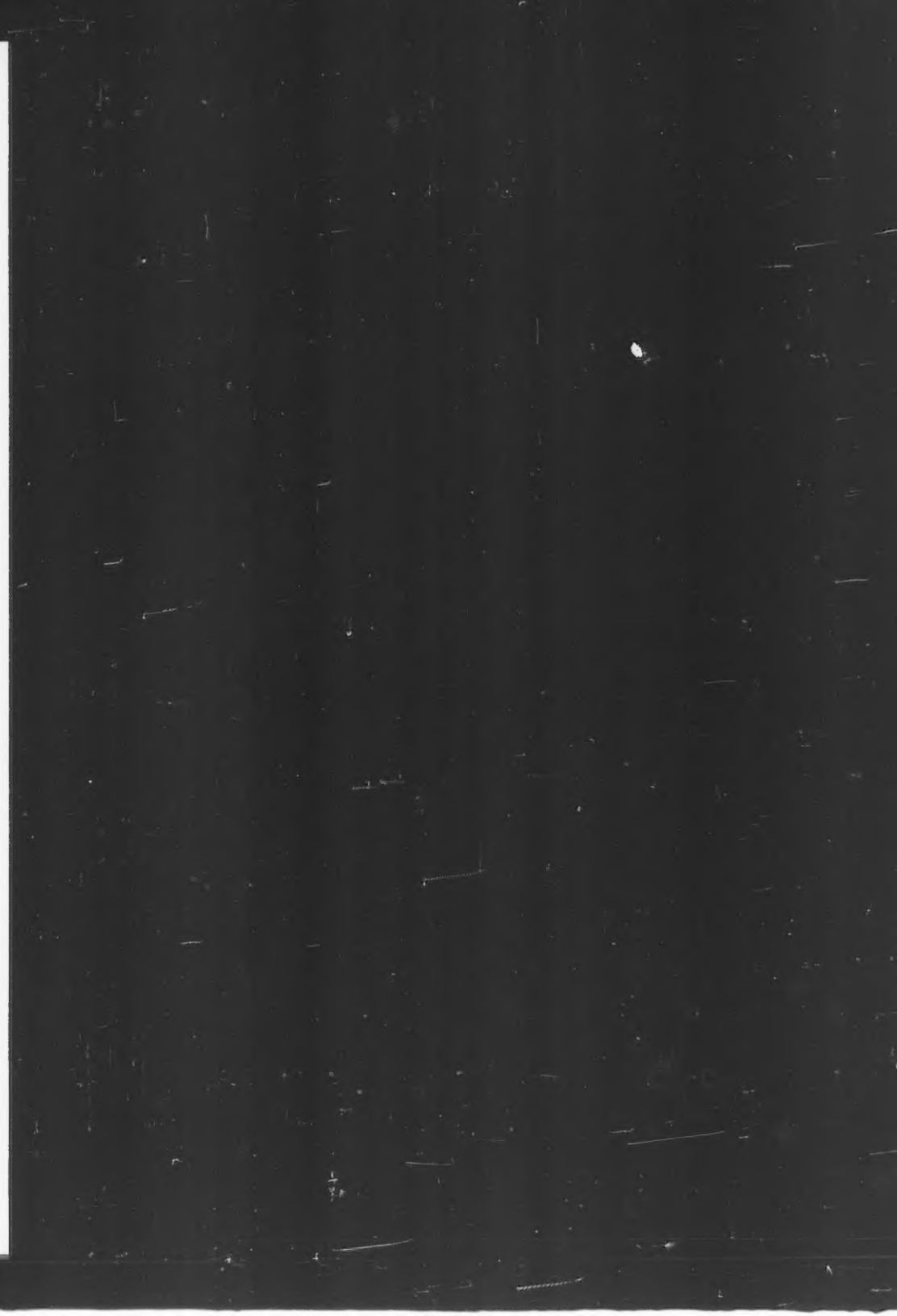
Zermatt-Saas zone, 545